PNAS
www.pnas.org

Supplementary Information for

Listeriolysin S: a bacteriocin from *Listeria monocytogenes* that induces membrane permeabilization in a contact-dependent manner

Jazmín Meza-Torres[a,b,c], Mickaël Lelek[d], Juan J Quereda[e], Martin Sachse[f], Giulia Manina[g], Dmitry Ershov[h,i], Jean-Yves Tinevez[h], Lilliana Radoshevich[j], Claire Maudet[k], Thibault Chaze[l], Quentin Giai Gianetto[l,m], Mariette Matondo[l], Marc Lecuit[c,k,n], Isabelle Martin-Verstraete[o], Christophe Zimmer[d], Hélène Bierne[p], Olivier Dussurget[a,c], Pascale Cossart[b] & Javier Pizarro-Cerdá[a1]

[1]Javier Pizarro-Cerdá e-mail: javier.pizarro-cerda@pasteur.fr

This PDF file includes:

Supplementary Material and Methods

Bacterial strains and growth conditions

Bacterial strains and plasmids used in this study are listed in Table S1 and Table S2. The *Lm* and *L. lactis* strains were grown in tubes overnight (ON) at 200 rpm and 37°C in BHI broth (Difco). When required, antibiotics were added for *Listeria* chloramphenicol 7 µg/mL and erythromycin 5 µg/mL.

Mutant and strains construction

Lm F2365 *ΔllsA* and *Lm* F2365 pHELP: *llsA* were constructed as indicated previously (1). Briefly, fragments of ~500-bp DNA flanking the *llsA* gene were amplified by PCR using the chromosomal DNA of *Lm* F2365 as template and ligated into the pMAD by using *Xma*I/*Sal*I restriction sites. All the primers used are listed in Table S3. For the construction of the *Lm* F2365 pHELP: *llsA* strain, the pHELP promoter (2) was fused between two 500-ntd DNA fragments flanking the start codon of *llsA* and the DNA construction was synthetically produced and cloned into SalI–EcoRI restriction sites of the the pMAD vector as indicated previously (1) .

For the strains *Lm* F2365 pHELP: *llsA*-FLAG and *Lm* F2365 pHELP: *llsA*-HA the FLAG and HA tags were added in the C terminal of the *llsA* gene and the pHELP promoter was fused between two 500-ntd DNA fragments flanking the start codon of *llsA.* These DNA constructions were synthetically produced by gene synthesis (Genecust) and cloned into *Sal*I–*Eco*RI restriction sites of pMAD vector. Mutagenesis was performed by double recombination as described previously (3). For the construction of the *llsGH* double mutant DNA constructions were synthetically produced by IDT and cloned into SalI-SmaI restriction sites of pMAD vector. Approximately 800 -ntd DNA fragments upstream and downstream of the *llsGH* genes were used to design the DNA blocks. Mutagenesis was performed by double recombination as described previously (3). For the construction of the strains expressing constitutively GFPmut2 and tdTomato, the fragments were cloned into the pAD vector as described previously (4). The tdTomato protein was codon optimized for its expression in *Lm* (http://genomes.urv.es/OPTIMIZER/).

Immunoprecipitation

Stationary phase cultures (1 L) of *Lm* F2365 pHELP: *llsA* and *Lm* F2365 pHELP: *llsA*-FLAG were pelleted. Bacteria were washed once with 50 mL of PBS and once with 50 mL of TS buffer. Bacteria were then resuspended into 25 mL of TS buffer containing 1250 µg mutanolysin (Sigma) and Complete protease inhibitor cocktail (Roche) ON statically at 37 °C to digest completely the cell wall. Protoplasts were pelleted 5 min at 15,000 *g*, resuspendend in 15 mL of CHAPS lysis buffer and lysed by four freeze-thaw cycles. The lysed protoplasts were sonicated (four cycles of 15 s, 20% amplitude). Samples were centrifuged 45 min at 4°C at 16,000 *g*. Supernatant was collected and 100 µL of equilibrated M2 anti-flag beads (Sigma, washed three times with 1 mL of CHAPS lysis buffer) were added to both lysates. The lysates were incubated ON at 4 °C on a rotating wheel. Beads were collected by centrifugation at 4 °C 1 min at 2,000 g and washed once with CHAPS lysis buffer and then three times with 5 mL of Elution buffer (50 mM Tris HCl pH 8.0, 150 mM NaCl and 2 mM $CaCl_2$). The FLAG tag protein was eluted by 3 serial elutions (150 µL twice and 100 µL once) with the 3x FLAG peptide diluted in Elution buffer (final concentration of 100 µg/mL). The eluted fractions were analyzed by western Blot.

Antibodies

The following primary antibodies were used: mouse monoclonal Alexa Fluor 647-conjugated HA antibody (Invitrogen), mouse monoclonal anti-flag (M2, Sigma), mouse monoclonal anti-HA (6E2, Cell Signaling Technology) and home-made mouse monoclonal anti Internalin A (L7.7) (5), rabbit polyclonal anti-ActA (R32) (6) or rabbit monoclonal anti-ActA (A16) (7), rabbit polyclonal anti-EF-Tu (R114) (8) and rabbit polyclonal anti-Internalin C (R134) (9). Goat anti-mouse and anti-rabbit IgG HRP-conjugated antibodies (Abcam) were used as secondary antibodies. The primary antibodies were used in a 1:1000 dilution with exception of EF-Tu (1:40000) and Internalin C (1:2000) and the conjugated antibodies were used in a 1:5000 dilution.

SDS–PAGE and western blotting
Samples after cellular fractionation or immunoprecipitation were analyzed similarly. Equal amounts of each sample or fraction were then diluted with 100 µL of 2x Tricine Sample Buffer (Biorad) and 125 mM DTT to be analyzed by SDS–PAGE and western blotting. Samples were boiled 5 min at 95 °C and centrifuged at 15,000 *g* for 5 min and 20 µL (for subcellular fractions controls) or 35 µL (for LLS with tags) were loaded onto a NuPAGE 4-12% Bis-Tris Precast Protein Gels (Invitrogen). The samples were separated in Nu PAGE MOPS SDS Running Buffer (for protein controls) or MES SDS Running Buffer (for LLS) at 130 V and transferred onto a polyvinylidene fluoride (PVDF) membrane using the iBlot Dry Blotting System (Invitrogen) at 20 V for 8 min. The membranes were blocked with 5% skim milk in PBS 1X with 1% Tween-20 (PBST) and the primary antibodies were incubated ON at 4 °C and the secondary antibodies at 37 °C during 1 h at room temperature. The proteins were revealed with the Pierce ECL 2 Western Blotting Substrate or SuperSignal West Femto Maximum Sensitivity Substrate (Fisher Scientific) if necessary and image with Amersham Imager 680 (GE) or BioRad ChemiDoc MP.

RNA extraction and quantitative Real-Time PCR
Total RNA was extracted as previously described (10). Briefly, *Lm* F2365 strains were grown in BHI until stationary phase (OD_{600nm} =1.5) and pellets were resuspended in 1 mL TRIzol reagent (Ambion), transferred to 2 mL Lysing Matrix tubes and lysed with a FastPrep apparatus (2 cycles of 45 s, speed 6.5). Tubes were centrifuged 5 min at 10 000 *g* for 10 min at 4 °C and the aqueous phase was transferred twice to an Eppendorf tube containing 200 µL of chloroform, lysates were shaken 30 s and incubated at room temperature for 10 min at room temperature and centrifuged 15 min at 13,000 × *g* at 4°C. The upper aqueous phase was removed and transferred to a new Eppendorf tube and RNA was precipitated by the addition of 500 µL Isopropanol and incubation at room temperature for 10 min. RNA was pelleted by centrifugation (10 min at 13,000 × *g* at 4°C). The supernatant was discarded and the pellet was washed twice with 75% ethanol. RNA pellets were resuspended in 40 µL water. Purified RNA (10 µg) was subjected to DNase treatment (Turbo DNase). cDNA was obtained by treating 500 ng of RNA with QuantiTect Reverse Transcription Kit following manufacturer's instructions. The quantitative Real-Time PCR was performed on CFX384 Touch Real-Time PCR Detection System (Bio-Rad) using SsoFast EvaGreen Supermix following manufacturer's instructions (Bio-Rad). Each reaction was performed in triplicate with 3 independent biological replicates. Data were analyzed by the ΔΔCt method. Gene expression levels were normalized to the *gyrA* gene.

Immunofluorescence staining for super resolution microscopy of intact bacteria
Bacteria were grown in BHI broth ON and the cultures were refreshed until bacteria reached and OD_{600nm} = 2. Strain *Lm* F2365 pHELP: *llsA*-HA was used to detect the LLS and the strain without the tag *Lm* F2365 pHELP: *llsA* was used as a negative control. Bacteria were pelleted for 5 min at 15,000 *g* and fixed with 3% paraformaldehyde in PBS for 10 min at room temperature. After fixation, bacteria were washed twice in PBS for 10 min at room temperature. Bacteria were pelleted 5 min at 7,000 *g* and blocked with PBS + 2% BSA for 1 h at room temperature on a rocking platform. Bacteria were incubated with the monoclonal Alexa Fluor 647-conjugated HA antibody (Invitrogen, diluted in PBS + 2% BSA) for 3 h at room temperature in the dark. Thereafter, bacteria were washed with PBS 5 times in order to minimize nonspecific signal from the coverslip. Bacteria were kept at 4°C in PBS until imaging.

Immunofluorescence staining for super-resolution microscopy of protoplasts
Bacteria were grown in BHI broth ON and the cultures were refreshed until bacteria reached and OD_{600nm} = 2. Strain *Lm* F2365 pHELP: *llsA*-HA was used to detect the LLS and the strain without the tag *Lm* F2365 pHELP: *llsA* was used as a negative control. Protoplasts were prepared as indicated previously for subcellular fractionation. Protoplasts were pelleted for 5 min at 15,000 *g* and fixed with 3% paraformaldehyde + 0.5 M sucrose in PBS for 10 min at room temperature. After fixation, protoplasts were washed twice in PBS for 10 min at room temperature. Protoplasts were pelleted 5 min at 7,000 *g* and blocked with PBS + 2% BSA for 1 h at room temperature on a rocking platform. Protoplasts were incubated with a monoclonal AlexaFluor 647-conjugated HA antibody

(diluted in PBS + 2% BSA) for 3 h at room temperature in the dark. After, protoplasts were washed with PBS 5 times. Bacteria were kept at 4°C in PBS until imaging.

PAINT and dSTORM microscopy: sample preparation and imaging process

A drop of fixed and stained bacteria, as previously explained (11), was attached on a poly-L-Lysine treated coverslip (diameter 18mm) at room temperature for 30 min. Later, the coverslip was washed once with PBS and the DAPI solution (1:1000 in PBS) was added for 2 min and washed twice with PBS. Then, large magnetic dynabeads (ThermoFisher Dynabeads^{TM} M-280 Streptavidin) (1:1000) were deposited and stuck on the coverslip. Finally, the coverslip was placed in a magnetic chamber (Chamlide CMB 35 mm Dish Type 1) filled with oxygen scavenger buffer for dSTORM as described before (12), and 100nM of Nile Red probes were added for PAINT imaging. The magnetic beads are used for real-time correction of spatial drift. These beads were imaged through the objective lens using a transmission light coming from a 810nm LED and imaged onto a second camera which does not interfere with the fluorescent emission path. Custom-written Python software was used to determine the subpixelic position of the magnetic beads, allowing to detect small displacements of the sample, and to control the position of a three-axis piezoelectric stage (Piezoconcept).

First a low-resolution image was acquired in the DAPI channel. For dSTORM imaging, a sequence of 20,000 images were acquired in the A647 channel, using 35 ms exposure time and an EM gain of 200. For PAINT imaging, 20,000 frames were acquired in the Nile Red channel on the same field of view, with an exposure time of 100 ms and the same EM gain. Single molecule localizations from both channels were obtained using the ImageJ plugin ThunderStorm (13). The localization tables were exported to Matlab software for analyzing distances between LLS clusters and the bacterial membrane.

LLS cluster detection and analysis from PAINT/dSTORM microscopy

To calculate the distance between LLS clusters and the bacterial membrane, individual protoplasts were manually selected based on the low-resolution DAPI image and the super-resolution PAINT image of the membrane. An ellipse was fitted to all Nile Red PAINT localizations for each selected protoplast. In the vicinity of each ellipse, A647 localizations were automatically detected and localizations appearing in successive frames were merged in order to generate a cluster (LLS cluster). We computed a centroid for each LLS cluster as the mass center of all its localizations. Finally, we calculated the signed Euclidean distances between the LLS clusters centroid(s) and the ellipse, with a negative sign added for clusters inside the ellipse. Chromatic aberrations between the Nile Red and AF647 channels were corrected using images of multicolor beads.

Preparation of LLS$^{+/-}$ extracts and inactivation of LLS$^{+/-}$ cells

For the preparation of LLS$^{+/-}$ extracts the *Lm* subcellular fractionation protocol was used as described previously (14) with a few modifications. The cell wall, membrane and cytoplasm compartments were separated from 250 mL of stationary phase culture (OD_{600} = 2). The bacteria were pelleted and supernatant (SN) was precipitated at -20°C ON with 16% of trichloroacetic acid(TCA). The bacterial pellet was washed once with 200 mL of PBS and once with 50 mL of TS buffer (10 mM Tris-HCl pH 6.9, 10 mM $MgCl_2$ and 0.5 M sucrose). Then the bacteria were resuspended in 10 mL of TS buffer containing 45 µg mutanolysin (Sigma) and cOmplete protease inhibitor cocktail (Roche) ON statically at 37 °C to digest completely the cell wall. Protoplasts were pelleted for 5 min at 15,000 *g* and the cell wall fraction was precipitated with TCA as indicated before for the supernatant. The protoplasts were lysed by four freeze-thaw cycles (liquid nitrogen and water bath at 37 °C) in 10 mL of protoplast buffer (100 mM Tris-HCl pH 7.5, 100 mM NaCl and 10 mM $MgCl_2$). The membrane and the cytoplasm fractions were centrifuged at 4 °C for 15 min at 16,000 *g*. The pellet corresponding to the membrane fraction was then resuspended in 10 mL of CHAPS lysis buffer (30 mM Tris-HCl pH 7.5, 150 mM NaCl and 1% CHAPS). The membrane fraction was sonicated (three cycles of 15 s, 20% amplitude). Extracts were kept at -20°C. For the co-culture assays 200 µL of each extract obtained from LLS$^{+/-}$ was used per condition.

To heat inactivate LLS$^{+/-}$ cells were incubated 15 min at 96°C and to UV kill LLS$^{+/-}$ cells were incubated in a GS Gene Linker UV Chamber (Bio-Rad) with the sterilization program before co-

culture with *L. lactis*. To kill $LLS^{+/-}$ with antibiotics erythromycin was added (5 µg/mL) 4 h before co-culture with *L. lactis* pTc-GFP. In all cases the equivalent to 5×10^7 $LLS^{+/-}$ bacteria was inoculated per condition.

Co-culture assays were performed for 24 h statically at 37 °C in microaerophilic conditions (6% O_2 and 5-10% CO_2) as previously described (1). Briefly, 5×10^7 target bacteria from ON cultures were inoculated into 5 mL of fresh BHI either alone, with LLS^+ or LLS^- extracts or inactivated cells as indicated. At 24 h after inoculation, cultures were serially diluted and plated on BHI and Oxford agar plates (Oxoid). Experiments were performed three times independently.

Microfluidics and time-lapse microscopy

The customized microfluidics device consists of a PDMS chip with channels connected to an inlet and an outlet tubing. The bacteria are trapped between a glass coverslip and a semi-permeable cellulose membrane (Spectra/Por 6 Dialysis Tubing 25 kDa MWCO, Spectrum) for the growth rate assays or an agarose pad (1.5% w/v low-melting point agarose) for the cell membrane permeabilization assays. Before closing the device 2 µL of a mixture (target-LLS^+ and target-LLS^-) were inoculated in opposite sides of the device to avoid cross contamination (5×10^8 bacteria were inoculated for each strain, except for the recovery assays the inoculum was doubled). Once the microfluidics device was assembled, the silicone tubing connected to the two inlet ports of the microfluidic device were fixed to 50 mL syringes. The bacteria were fed by pumping the medium into the tubing, and by diffusion of the medium from the channels of the PDMS device through the membrane. For the growth rate assays BHI broth was pumped using a syringe pump set at a rate of 25 µL/min during 10 h, and for the cell membrane permeabilization assays BHI broth was pumped during 3 h and then changed to PBS 1x (Dulbeco PBS Gifco) with Blue Sytox dye (final concentration 1 µM) during 10 h. For the recovery assays BHI was pumped during 2 h, changed to PBS with Blue Sytox dye for 2 h and then the cycle was repeated once again.

Microfluidics image analysis

To measure GFP signal dynamics and SYTOX uptake dynamics in target cells, we defined a set of regions of interest (ROI). First, the signal ROI (sROI) includes target cells that are in direct contact with producer cells (LLS^+) or *llsA* mutant cells (LLS^-); sROI signal reports the contact-dependent inhibition effect. Second, the reference ROI (rROI) includes target cells close to sROI but not in direct contact with LLS^+ or LLS^- (deeper into the microcolony); rROI signal reports the basal target microcolony signal. In addition, we defined a focus ROI (fROI) to include only those areas of an image that are focused.

To extract the sROI and the rROI, the microcolonies were smoothed (gaussian blur) and segmented (auto-threshold function, mode IsoData) using FIJI (15). Next, morphological operations were used (FIJI plugin MorpholibJ) (16) to extract the sROI and rROI. Briefly, the segmented $LLS^{+/-}$ microcolonies are dilated to get the external rim (mask 1) and the target bacteria microcolonies are eroded to get the inner rim (mask 2). The intersection between these rims gives the sROI (mask 3). The same procedure was used to get the rROI (mask 4), but to set it deeper into the target microcolony (further from the producer) we use a larger size for dilation and erosion. The size used for dilation/erosion was 25 pixels (sROI) and 50 pixels (rROI). The width of the rim for sROI and rROI was limited to 25 pixels (length of one bacterial cell in our acquisition conditions).

Once the ROIs were identified, we calculated the fluorescence intensity (maximum signal intensity for GFP and the mean signal intensity for SYTOX) in these ROIs, and then the ratio (R) between them (R= sROI/rROI). If R is close to 1, the signal of the contact area is similar to the reference area, suggesting that target cells keep their integrity (for SYTOX) or there is no accumulation of the GFP protein. If R is >1 the signal is stronger in the area of contact, suggesting that there is membrane permeabilization (for SYTOX) and there is accumulation of GFP protein inside the target cells. The analyses were done for each time lapse with single values at each time point. The mean and the standard deviation were calculated for each time point.

To compare the growth rate of the target microcolonies as opposed to the producer or *llsA* mutant microcolonies, the relative microcolony area (RMA) was calculated. Briefly, the microcolonies were segmented and the area was normalized to the full area of the field of view 1024 x 1024 pixels to get the RMA. If both microcolonies grew at the same rate the average area of both microcolonies will occupy half of the field of view with RMA equal to 0.5.

To calculate the growth rate of bacteria in different conditions manual segmentation was performed using Icy software (17). A polygon (ROI) was drawn around a bacterium of interest to get its perimeter and the cell planar area (μm^2) (obtained from sum of the size of pixels within the ROI). The single bacterial growth rate was calculated by fitting an exponential curve to sequential size measurements of the ROIs over the lifetime of the cell as described before (18). Briefly, the values were fitted to a nonlinear regression, exponential growth equation (using Prism 8.0) to obtain the doubling time in minutes and the growth rate k (min^{-1}).

Click chemistry and flow cytometry analyses

Target bacteria were incubated with 1 mM 3-Azido D-alanine ($C_3H_6N_4O_2$.HCl dissolved in DMSO) ON. Bacteria were washed twice in PBS and co-cultured with LLS^- or LLS^+ cells for 3 or 5 h in BHI (as previously mentioned). After, the co-culture was pelleted and cells were fixed with 200 µL ice cold pure methanol during 2 min. The samples were diluted with 200 µL cold PBS. Bacteria were centrifuged 3 min at 13,000 × *g* at 4°C and half of the supernatant was removed and replaced with cold PBS three times. Then tubes were centrifuged 3 min at 13,000 × *g* at 4°C and pellets were resuspended in 200 µL of PBS + 1% Bovine Serum Albumin. Samples were labelled with Click-iT® Cell Reaction Buffer Kit following manufacturer's instructions. Briefly, bacteria were resuspended in 200 µL reaction cocktail with or without (control mix) 500 µM of Alexa Fluor 594-alkyne. Samples were incubated 30 min in the dark at room temperature and bacteria were washed twice by centrifugation with PBS + 1% Bovine Serum Albumin. Bacteria were resuspended in PBS and diluted to perform flow cytometry analyses. Samples were acquired in a Cytoflex S (Beckman Coulter) and data were analyzed with FlowJo. Green Fluorescence was collected from 40 000 FSC/SSC-gated bacterial events in the FITC channel (525nm/40 nm bandpass filter). Fluorescence intensities were plotted in single-parameter histograms that were normalized to mode for the two populations (target bacteria incubated with LLS^- or LLS^+ after 3 or 5 h of co-culture).

Detection of extracellular ATP

Extracellular ATP levels of co-cultures were measured by using a ATP Fluorometric Assay Kit (Abcam) following manufacturer's instructions. Briefly, co-culture filtered supernatants were deproteinized with 10kD Amicon Membrane Ultracel-10 (Merck) by centrifuging at 13,000 *g* for 15 min at 4°C. The filtrate was collected and 1:10 dilutions were prepared to reduce the fluorescence background. Background ATP was blanked using sterile 1:10 diluted deproteinized BHI. Samples were analyzed after 30 min of reaction in black walled, clear bottom 96-well plates by using a GloMax® Discover Microplate Reader by using the Green filter (Ex 520 nm, Em 580-640).

Flow cytometry and cell sorting

After 4 hours of co-culture bacteria were centrifuged, washed once and resuspended in PBS. GFP target bacteria were purified with a FACSAria III (Becton Dickinson), a nozzle of 70 µm was used. Bacteria were positively selected at 4°C with the FITC channel (530nm/40nm bandpass filter) collecting a maximum 10 000-FSC/SSC-gated bacterial events per second in a 15 mL tube. Approximately 1 x 10^8 bacteria were isolated after 5 hours. Collected bacteria were centrifuged, washed twice and resuspended in 250 µL of HEPES buffer (20 mM HEPES pH 8.0, 1 mM $MgCl_2$) in low binding eppendorf tubes. Approximately 25 ng of mutanolysin was added to each suspension and samples were incubated for 1hr at 37˚C. Urea was added dry to both samples to a final concentration of 8 M. Lysates were sonicated by four bursts of 15 seconds at an amplitude of 20%. Then, lysates were cleared by centrifugation for 15 min at 16 000g at RT. The protein concentration in the supernatants was measured by BCA. Experiments were performed four times for each condition, independently.

Mass spectrometry-based proteomics

Equal amount of proteins from target bacteria exposed to LLS^+ or LLS^- were precipitated by using a TCA-Acetone approach. Briefly, a volume of ice-cold TCA was added to the sample, vortex and 1 volume of ice-cold acetone was added. Samples were incubated at 4°C for 30 min and proteins were pelleted at 16 000 g for 15 min at 4°C. Resulting pellet was washed twice in ice-cold acetone and spin down. Remaining acetone was removed under hood. Pellet of proteins was resuspended in ammonium bicarbonate 50 mM and reduced using TCEP 10mM for 30 min at RT with sonication steps. Alkylation of reduced disulfide bridges was done using iodoacetamide 20mM for 30 min at room temperature in the dark. Digestion of protein was performed using 500 ng of trypsin (Promega) and performed at 37°C overnight. Digestion was stopped adding 1% final of TFA and resulting peptides were desalted using homemade stage tips and lyophilized until further LC-MS analysis. Peptides were resuspended in loading buffer (0.1% FA). LC-MS/MS analysis of digested peptides was performed on an Orbitrap Q Exactive Plus mass spectrometer (Thermo Fisher Scientific, Bremen) coupled to an EASY-nLC 1200 (Thermo Fisher Scientific). A home-made column was used for peptide separation (C18 40 cm capillary column picotip silica emitter tip 75 µm diameter filled with 1.9 µm Reprosil-Pur Basic C18-HD resin, Dr. Maisch GmbH, Ammerbuch-Entringen, Germany). The column was equilibrated and peptide were loaded in solvent A (0.1 % FA) at 800 bars. Peptides were separated at 250 $nl.min^{-1}$. Peptides were eluted using a gradient of solvent B (ACN, 0.1 % FA) from 3% to 22% in 140 min, 22% to 42% in 61 min, 42% to 60% in 15 min, 60% to 75% in 15 min (total length of the chromatographic run was 240 min including high ACN level steps and column regeneration). Mass spectra were acquired in profile mode in data-dependent acquisition mode with the XCalibur 2.2 software (Thermo Fisher Scientific, Bremen) with automatic switching between MS and MS/MS scans using a top-10 method. MS spectra were acquired at a resolution of 70000 (at m/z 400) with a target value of 3×10^6 ions. The scan range was limited from 200 to 2000 m/z. Peptide fragmentation was performed using higher-energy collision dissociation (HCD) with the energy set at 26 NCE. Intensity threshold for ions selection was set at 1×10^6 ions with charge exclusion of $z = 1$ and $z > 7$. The MS/MS spectra were acquired in profile mode at a resolution of 17500 (at m/z 400). Isolation window was set at 1.6 Th. Dynamic exclusion was employed within 35s.

Acquired MS data were searched using MaxQuant (version 1.5.3.8) (with the Andromeda search engine) against a home-made database of the proteome of *Listeria monocytogenes* 10403S. The following search parameters were applied: carbamidomethylation of cysteines was set as a fixed modification, oxidation of methionine and protein N-terminal acetylation were set as variable modifications. The mass tolerances in MS and MS/MS were set to 5 ppm and 20 ppm respectively. Maximum peptide charge was set to 7 and 7 amino acids were required as minimum peptide length. Two miss cleavages for trypsin were allowed. A false discovery rate of 1% was set up for both protein and peptide levels.

Statistical analyses of protein intensities

Quantification of each identified protein was performed by summing the intensities of its associated peptides if at least 1 unique peptide was identified per protein. For the statistical analysis of one condition versus another, proteins identified in the reverse and contaminant databases and proteins “only identified by site” (with an identification score too low - not exceeding the 1% FDR threshold) were first discarded from the list. Then, proteins exhibiting fewer than 2 summed intensities in at least one condition were discarded from the list to avoid misidentified proteins. After log2 transformation of the leftover proteins, summed intensities were normalised by median centering within conditions (wrapper.normalizeD function of the R package DAPAR) (19). Remaining proteins without any summed intensities in one of both conditions have been considered as proteins present in a condition and absent in another. They have therefore been set aside and considered as differentially abundant proteins. Next, missing values were imputed using the impute.slsa function of the R package imp4p (20). Proteins with a fold-change inferior to 1.5 (log2(FC) inferior to 0.58) have been considered as proteins which are not significantly differentially abundant. Statistical testing of the remaining proteins (having a log2 (fold-change) superior to 1) was conducted using a limma t-test thanks to the R package limma (21). An adaptive Benjamini-Hochberg procedure was applied on the resulting p-values thanks to the function adjust.p of R package cp4p (22) using

the robust method of Pounds and Cheng (2006) to estimate the proportion of true null hypotheses among the set of statistical tests (23). The proteins associated to an adjusted p-value inferior to a FDR level of 1% have been considered as significantly differentially abundant proteins. Finally, the proteins of interest are therefore those which emerge from this statistical analysis supplemented by those which are considered to be absent from one condition and present in another.

Extraction of LLS hemolytic fractions with LTA

Partial purification of LLS was carried out as described before for SLS (24). Briefly, *Lm* F2365 pHELP: *llsA ∆hly* (LLS^+), *Lm* F2365 pHELP: *llsA*-FLAG *∆hly* and *Lm* F2365 ∆*llsA* ∆*hly* (LLS^-) were grown ON at 37°C in BHI supplemented with maltose (1% w/v) and sodium bicarbonate (2% w/v; BHI-BM). 10 mL of this culture was inoculated in 500 mL of BHI-BM and grown at 37°C for 5 h. The culture was centrifuged, the cell free supernatant collected for assessment of hemolysis. The cell pellet was washed in 100 mM potassium phosphate buffer pH 7 before resuspension to a final volume of 8 mL in induction buffer (IB; 100 mM KH_2PO_4, 2 mM $MgSO_4$, 30 mM maltose, pH 7). The cell suspension was centrifuged and 1 mL of the cell free supernatant was also collected for assessment. The remaining 7 mL volume of cell suspension was incubated at 37°C for 5 min before being induced during 5 min through the addition of 3.5 mg of Lipoteichoic acid from *S. aureus* (LTA, Sigma) and immediately centrifuged. The induced and not induced supernatants were filtered and supplemented with ammonium acetate (AmAc; 100 mM, pH 7). Hemolytic activity was assessed through the creation of wells (4.6 mm diameter, 200 µL tips diameter) in Columbia blood agar plates (5% sheep's blood) and the introduction of 50 µL to be assessed. Plates were incubated ON at 37°C. The remaining induced supernatant fractions were used for immunoprecipitation as indicated previously.

Table S1. Strains used in this study

Strains	Description	Source	BUG or CIP
L. monocytogenes F2365	Strain associated with the California 1985 listeriosis outbreak	(25)	BUG 3012
L. monocytogenes F2365 Δ*llsA*	Deletion of the *llsA* gene	(1)	BUG 3781
L. monocytogenes F2365 Δ*llsA* Δ*hly*	Deletion of the *llsA* gene and the *hly* gene	(26)	BUG 3828
L. monocytogenes F2365 Δ*llsB*	Deletion of the *llsB* gene	(1)	BUG 3668
L. monocytogenes F2365 pHELP: *llsA*	Strain that expresses the LLS operon constitutively under the control of the pHELP promoter	(1)	BUG 3817
L. monocytogenes F2365 pHELP: llsA Δhly	Strain *L. monocytogenes* F2365 pHELP: *llsA* where the *hly* gene was deleted	(26)	BUG 3819
L. monocytogenes F2365 pHELP: *llsA* Δ*llsB*	Strain *L. monocytogenes* F2365 pHELP: *llsA* where the *llsB* gene was deleted	This study	BUG 4314
L. monocytogenes F2365 pHELP: *llsA*-FLAG	Strain that expresses the LLS operon constitutively under the control of the pHELP promoter. The FLAG tag was added in the C terminal of the *llsA* gene.	This study	BUG 4177
L. monocytogenes F2365 pHELP: *llsA*-FLAG *Δhly*	Strain *L. monocytogenes* F2365 pHELP: *llsA*-FLAG where the *hly* gene was deleted	This study	BUG 4178
L. monocytogenes F2365 pHELP: *llsA*-HA	Strain that expresses the LLS operon constitutively under the control of the pHELP promoter. The HA tag was added in the C terminal of the *llsA* gene.	This study	BUG 4179
L. monocytogenes F2365 pHELP: *llsA*-FLAG Δ*llsB*	Strain *L. monocytogenes* F2365 pHELP: *llsA*-FLAG where the *llsB* gene was deleted	This study	BUG 4315
L. monocytogenes F2365 Δ*llsGH*	Strain *L. monocytogenes* F2365 where the *llsGH* genes were deleted	This study	BUG4320
Lactococcus lactis lactis	Strain from the Institut Pasteur collection		CIP 70.56T
L. lactis pTc-GFP	Strain CIP 70.56T with the plasmid pTCVΩ*gfp*	This study	4306
L. monocytogenes 10403S	Lineage II strain commonly used in laboratories (it lacks the LLS operon)	(27)	BUG 1361
L. monocytogenes EGD	Lineage II strain commonly used in laboratories (it lacks the LLS operon)	(28)	BUG 600
L. monocytogenes EGD Δ*dltA*	EGD *dltA* (LMON_0982) deletion mutant	(29)	BUG 2182
L. monocytogenes F2365 Δ*llsA* pAD-tdTomato	*L. monocytogenes* F2365 Δ*llsA* with tdTomato inserted into the chromosome using the plasmid pAD.	This study	BUG4339
L. monocytogenes F2365 pHELP: *llsA* pAD-tdTomato	*L. monocytogenes* F2365 pHELP: *llsA* with tdTomato inserted into the chromosome using the plasmid pAD.	This study	BUG4340
L. monocytogenes 10403S pAD-cGFP	*L. monocytogenes* 10403S with cGFP inserted into the chromosome using the plasmid pAD.	This study	BUG 4208

Table S2. Plasmids used in this study

Plasmids	Description	Source	BUG no.
pMAD	Shuttle vector used for mutagenesis	(3)	BUG1957
pMAD-llsA	Plasmid used to create the deletion Δ*llsA* mutant	(1)	BUG 3751
pMAD-llsB	Plasmid used to create the deletion Δ*llsB* mutant	(1)	BUG3668
pMAD-pHELP: llsA	Plasmid used to insert the pHELP promoter into the upstream region of the LLS operon	This study	BUG3801
pMAD-pHELP: llsA-FLAG	Plasmid used to insert the FLAG tag into the C terminal of the *llsA* gene	This study	BUG4142
pMAD-pHELP: llsA-HA	Plasmid used to insert the HA tag into the C terminal of the *llsA* gene	This study	BUG4143
pPL2	*L. monocytogenes* site-specific phage integration vector	(4)	BUG2176
pAD-GFPmut2	pPL2-P*hyper*-GFP (constitutive)	(4)	BUG2479
pAD-tdTomato	pPL2-P*hyper*-tdTomato (constitutive)	This study	BUG4337
pTCVΩ*gfp*	EGFP expression vector	(30)	4448

Table S3. Primers used in this study

Name	Sequence 5'-3'	Purpose
llsAtag F	gcatattatcaaacggagggata	Verification of the tag insertion
llsAtag R	ctttcaagttcatatttgtgta	Verification of the tag insertion
pmad up	aagcgagaagaatcataatgg	Sequencing of the pMAD inserts
Pmad down v2	cataattattccccctagctaattttcgt	Sequencing of the pMAD inserts
llsB mut Fw	gtcaatatactgtttggct	Verification of the *llsB* gene mutation
llsB mut Rv	acagagaagattgaccat	Verification of the *llsB* gene mutation
llsGH clon Fw	atgccatggtacccgggatggtaataag	Amplification of DNA insert to clone into pMAD
llsGH clon Rv	catatgacgtcgacgtggttgattgtaagt	Amplification of DNA insert to clone into pMAD
llsGH pHELPFw	gcaattcactcgagatctgcaggat	Amplification of DNA insert to clone into pMAD
llsGH pHELP Rv	taggttgcgtctcgagtcaaatgcct	Amplification of DNA insert to clone into pMAD
Mut GH F	atgatgagcgtaacgcta	Verification of the *llsGH* gene mutation
Mut GH R	tccatggtttcgtataca	Verification of the *llsGH* gene mutation
pPL2-Fw	ttcgacccggtcgtcggttc	Sequencing insert in pAD-based plasmid
pPL2-Rv	cttagacgtcattaaccctcac	Sequencing insert in pAD-based plasmid
NC16	gtcaaaacatacgctcttatc	Verification of the plasmid integration into the chromosome
PL95	acataatcagtccaaagtagatgc	Verification of the plasmid integration into the chromosome
gyrA-RT-PCR-F	gcgatgagtgtaattgttg	For quantitative Real-Time PCRs
gyrA-RT-PCR-R	atcagaagtcatacctaagtc	For quantitative Real-Time PCRs
llsA-RT-PCR-F	tcacaatcatcaaatggctaca	For quantitative Real-Time PCRs
llsA-RT-PCR-R	caagaacatgagcaacatcca	For quantitative Real-Time PCRs
llsG-RT-PCR-F	gagagagcgcagtttttacaca	For quantitative Real-Time PCRs
llsG-RT-PCR-R	tcgttgtttttctccaccag	For quantitative Real-Time PCRs
llsH-RT-PCR-F	cccggatattgatgccagta	For quantitative Real-Time PCRs
llsH-RT-PCR-R	ggaagttccgaaaaagatgaaa	For quantitative Real-Time PCRs
llsX-RT-PCR-F	ttcacatgaatgatggcaca	For quantitative Real-Time PCRs
llsX-RT-PCR-R	ttcccaccatctcactacca	For quantitative Real-Time PCRs
llsB-RT-PCR-F	ggcaattcaccaatgctagg	For quantitative Real-Time PCRs
llsB-RT-PCR-R	tccatttctcttgcctcgtt	For quantitative Real-Time PCRs
llsY-RT-PCR-F	acatggagaaactggctgct	For quantitative Real-Time PCRs
llsY-RT-PCR-R	caaacatcaattcagctgtgg	For quantitative Real-Time PCRs
llsD-RT-PCR-F	ggatgcctttgcaatttgtt	For quantitative Real-Time PCRs
llsD-RT-PCR-R	gcagtgcctgttgatacagc	For quantitative Real-Time PCRs
llsP-RT-PCR-F	acagtttgtggtagttttatcgc	For quantitative Real-Time PCRs
llsP-RT-PCR-R	tcacgaatgaaaaggtggct	For quantitative Real-Time PCRs

Table S4. Upregulated (green) or exclusively expressed proteins (blue) in the target bacteria after co-culture with LLS^+ when comparing to co-culture with LLS^-.

LMRG	Name	Function
ATP production		
00411	Pyruvate oxidase	Pyruvate + phosphate + O_2 <=> Acetyl-P + CO_2 + H_2O_2 EC 1.2.3.3
00819	Phosphate butaryl transferase	Butanoyl CoA +phosphate= CoA + butyrylyl phosphate EC 2.3.1.19
00820	Butyrate kinase	ADP + butyryl-phosphate= ATP + butyrate EC 2.7.2.7
00119	Fructose-specific PTS IIB	Phosphorylated by phospho-IIA, before the phosphoryl group is transferred to the sugar substrate.
01787	RNA polymerase sigma-54 factor	Regulation of PTS activity, alteration of the pyruvate pool and modulation of carbon catabolite regulation(31) Also involved in osmotolerance (32)
01929	MurR/RpiR family transcriptional regulator	Regulators of genes involved in phosphor-sugar metabolism. Such as the conversion of ribose-5-phosphate (R5P) and ribulose-5-phosphate (Ru5P) (EC 5.3.1.6). Pentoses phosphate pathway can generate Fructose-6-P
02403	Sugar-phosphate phosphohydrolase	sugar phosphate + H2O = sugar + phosphate Acts on fructose 1,6-bisphosphate EC 3.1.3.23
02599	Cof-type HAD-IIB family hydrolase	sugar phosphate + H2O = sugar + phosphate Acts on fructose 1,6-bisphosphate EC 3.1.3.23
02442	Cytochrome aa3 quinol oxidase subunit II	This enzyme catalyzes the oxidation of quinol with the concomitant reduction of molecular oxygen to water. This acts as the terminal electron acceptor in the respiratory chain.
02001	Dihydroxyacetone kinase subunit L PTS dependent DhaL	A multi-subunit form with a phosphoprotein donor related to PTS transport proteins. The dihydroxyacetone kinase of *Escherichia coli* utilizes a phosphoprotein instead of ATP as phosphoryl donor (33) EC 2.7.1.121
02819	PuuD Gamma-glutamyl-gamma-aminobutyrate hydrolase	4-(gamma-glutamylamino)butanoate + H_2O = 4-aminobutanoate + L-glutamate EC 3.5.1.94
Methyl-glyoxal pathway		
02083	Glutathione peroxidase	Reduction of hydroxyperoxides Reduction of lipid peroxydes EC 1.11.1.9 2 glutathione + H_2O_2 <=> glutathione disulfide + 2 H_2O
00560	Glyoxalase/Bleomycin resistance protein	Lactoylglutathione lyase (also called glyoxalase I) catalyzes the first step of the glyoxal pathway. S-lactoylglutathione is then converted by glyoxalase II to lactic acid EC 4.4.1.5 (R)-S-lactoylglutathione = glutathione + 2-oxopropanal
01675	MBL fold metallo-hydrolase	Hydroxyacylglutathione hydrolases (also called glyoxalase II) which hydrolyze S-d-lactoylglutathione to d-lactate in the second step of the glycoxlase system EC 3.1.2.6

Amino acids production		
01434	Prephenate dehydratase	Prephenate = phenylpyruvate + H_2O + CO_2 can regenerate $NADH^+H^+$ Phe Tyr and Trp metabolism EC 4.2.1.51
02719	Aspartate kinase	ATP + L-aspartate = ADP + 4-phospho-L-aspartate Gly Ser and Thr metabolism EC 2.7.2.4
02585	Pyridoxal phosphate-dependent aminotransferase	Carbohydrates and nitrogen metabolism Methionine salvage pathway EpsN (EC:2.6.1.-) biosynthesis of amino acids and amino acid-derived metabolites
Purine and pyrimidine salvage pathways		
01055	Putative pyrophosphatase MazG domain	ATP + H2O = AMP + diphosphate EC3.6.1.8 Also acts on ITP, GTP, CTP and UTP.
00685	RdgB	Purine non-canonical NTPase hydrolyze nonstandard nucleotides such as XTP to XMP and ITP to IMP. EC 3.6.1.66
01112	ADP-ribose pyrophosphatase	catalyzes the hydrolysis of ADP-ribose and a variety of additional ADP-sugar conjugates to AMP and ribose-5-phosphate. EC 3.6.1.13
02064	Adenylate cyclase	Acts on dATP to form 3',5'-cyclic dAMP EC 4.6.1.1
Stress response		
01103	Fur family transcriptional regulator	Regulation of iron conditions iron uptake repressor is a transcription factor which utilizes Fe^{2+} as a corepressor and represses siderophore synthesis in pathogens. Fur, directly or indirectly, controls expression of enzymes that protect against ROS damage (34).
01869	Nitroreductase domain-containing protein FMR2	Metabolize nitro substituted compounds such as RNS. This process requires NAD(P)H as electron donor in an obligatory two-electron transfer and uses FMN as cofactor. Involved in oxidative stress response
00927	Protein GrpE	Co-chaperone with capacity to stabilize proteins in their folded states under denaturing stress conditions.
01165	Cold shock protein CspB	Indispensable for cold shock and osmotic stress Nucleic acid chaperone
00814	Cold shock-like protein CspC	In response to environmental stresses. Possess an RNA binding site.
Flagella and chemotaxis		
00405	FliI	Flagellar protein export ATPase for motor rotation
00404	FliH	Flagellum specific export
00412	Methyl-accepting chemotaxis protein	Transduce the signal to swim towards nutrients and away from toxins.
00403	FliG	Flagellar motor switch protein.
00378	Flagellin	Polymerize flagellin to form flagella.

Table S5. Exclusively expressed proteins (red) in the target bacteria after co-culture with LLS^- when comparing to co-culture with LLS^+.

LMRG	Name	Function
ATP utilization/metabolism		
00766	Phosphatidate cytidylyltransferase	Catalyzes the synthesis of CDP-diacylglycerol from cytidine triphosphate and phosphatidate. EC 2.7.7.41
00833	Acylphosphatase	Acyl-P + H_2O = carboxylate + P EC 3.6.1.7
01290	MenA (DHNA-octaprenyltransferase)	Trans-polyprenyl diphosphate + 1,4-dihydroxy-2-naphthoate = demethylmenaquinol + diphosphate + CO_2 EC 2.5.1.74
02507	PurD	ATP + 5-phospho-D-ribosylamine + glycine = ADP + phosphate + N1-(5-phospho-D-ribosyl)glycinamide EC 6.3.4.13
02504	PurM	ATP + 2-(formamido)-N1-(5-phospho-D-ribosyl)acetamidine = ADP + phosphate + 5-amino-1-(5-phospho-D-ribosyl)imidazole EC 6.3.3.1
01041	Nth Endonuclease III	The C-O-P bond 3' to the apurinic or apyrimidinic site in DNA is broken, leaving a 3'-terminal unsaturated sugar and a product with a terminal 5'-phosphate EC 4.2.99.18
01757	Hydrolase	
02066	GTP pyrophosphokinase	
00547	CDP-ribitol:polyribitol phosphotransferase	CDP-ribitol + (ribitol phosphate)n = CMP + (ribitol phosphate)n^+1
01897	Oxidoreductase	
00982	CarB Carbamoyl-phosphate synthase	Catalyzes the reaction of ATP and bicarbonate to produce carboxy phosphate and ADP EC 6.3.5.5
01565	Fumarylacetoacetate hydrolase	Catalyzes the final step in the catabolism of 4-fumarylacetoacetate and water into acetoacetate, fumarate, and H^+ respectively.
01850	Phosphatidylglycerophosphatase A	Lipid phosphatase which dephosphorylates phosphatidylglycerophosphate (PGP) to phosphatidylglycerol (PG)
01431	GlpF Glycerol uptake facilitator protein	Transporter of glycerol across the cytoplasmic membrane, with limited permeability to water and small uncharged compounds such as polyols.
02132	Morphine 6-dehydrogenase	Alkaloid degradation
01306	Radical SAM protein	Heme chaperone insert heme into respiratory enzymes
01374	NifS/IcsS protein	Class-V pyridoxal-phosphate-dependent aminotransferase family.
ABC transporters		
02524	ABC transporter domain-containing protein	
01618	ABC-2 type transport system permease	

02145	EcfA Energy-coupling factor transporter ATP-binding protein	Non-canonical ABC transporter
02143	EcfT Energy-coupling factor transporter transmembrane protein	Non-canonical ABC transporter
Stressosome		
01324	RsbR protein	
02314	RsbT antagonist protein rsbS	
Regulator		
01748	Phosphate regulon sensor histidine kinase PhoR	Phosphate homeostasis regulator
Others		
02556	Rod shape-determining protein MreB	
02307	Membrane protein	
00936	ComE operon protein 2	Competence regulator
00721	Signal peptidase I	Cleavage of hydrophobic, N-terminal signal or leader sequences EC 3.4.21.89

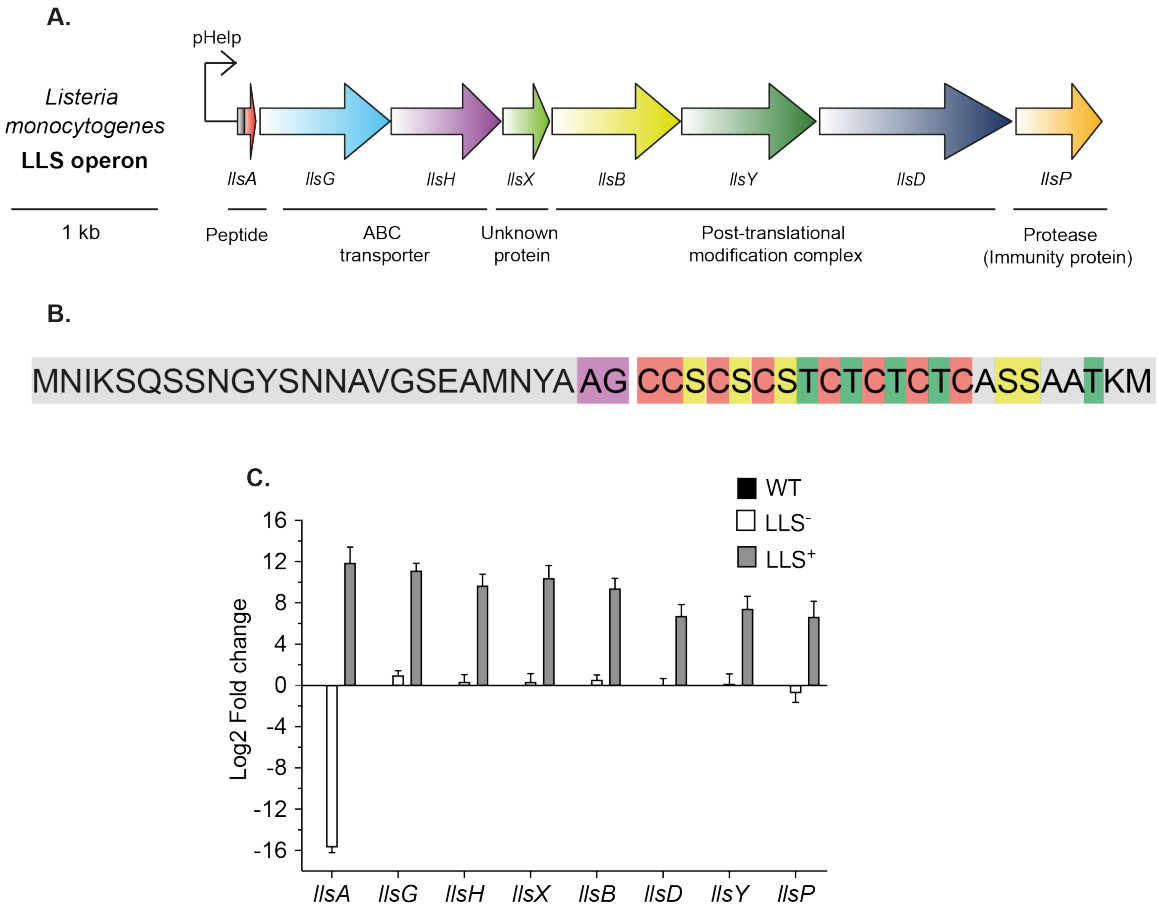

Figure S1. Operon organization, amino acid sequence and transcription of LLS operon genes in the LLS$^+$ and LLS$^-$ strains. (A) The gene cluster organization of LLS in *Lm.* The putative genes are indicated by colors as follows: in red the precursor peptide; in light blue, purple the ABC transporter genes; in light green the CAAX protease; in yellow the dehydrogenase gene; in dark green the cyclodehydratase gene; in dark blue the docking gene; and in turquoise the immunity gene. The light green (*llsX*) is a *Listeria* unique gene of unknown function. Upstream of the LLS operon the constitutive promoter pHelp is represented. (B) Amino acid sequences of Listeriolysin S precursor (LlsA). The predicted leader region is to the left (represented in gray) and terminate in putative leader cleavage sites (purple). Residues that are putatively modified are indicated in red (Cys), yellow (Ser) and green (Thr). Non-modified amino acids are shown in light gray. (C) Expression of the LLS genes *in vitro* upon introduction of the strong constitutive promoter pHELP upstream of the *llsA* gene (LLS$^+$) or mutation of the *llsA* gene (LLS$^-$) in the *wt* strain. Values calculated by qPCR in comparison with the *wt* strain and normalized to the housekeeping gene *gyrA* represented as Log2 Fold change. Data from three independent biological experiments performed with three technical replicates are shown. Error bars show SEM.

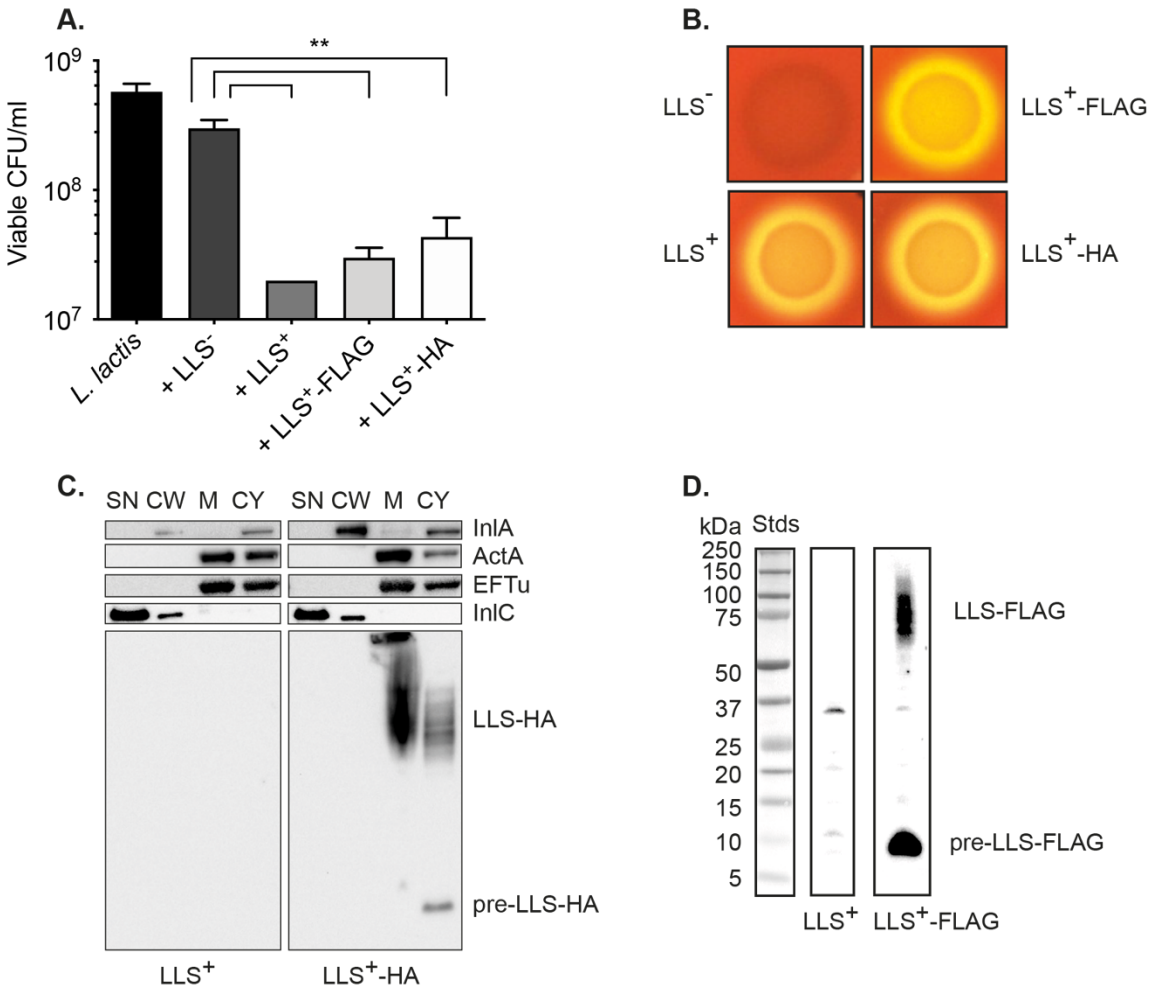

Figure S2. **LLS activity and subcellular localization upon addition of FLAG and HA tags.** (A) Target *L. lactis* bacteria were cultivated alone or co-cultivated with LLS mutant bacteria (LLS^-), LLS producer bacteria (LLS^+) or LLS producer bacteria with tags (LLS^+-FLAG and LLS^+-HA) during 24 h in BHI. Data from three independent biological experiments are shown. Error bars show SEM. Multiple two-tailed unpaired *t*-test were performed, LLS^- vs LLS^+ p= 0.0041, LLS^- vs LLS^+-FLAG p= 0.0048 and LLS^- vs LLS^+-HA p= 0.0070 (B) Assessment of hemolytic activity present in LLS^-, LLS^+, LLS^+-FLAG and LLS^+-HA strains in Columbia agar + 5% sheep blood. (C) Localization of LLS by fractionation experiments. Western Blot analysis was performed on a strain expressing LLS^+ (negative control) and a strain expressing LLS^+-HA (HA at the C-terminus). Proteins were fractionated in four compartments supernatant (SN), cell wall (CW), membrane (M) and cytoplasm (CY). InlA, ActA, EF-Tu and InlC were used as controls for fractionation. Pre-LLS FLAG indicates the unmodified LLS peptide. (D) Complete lysates of LLS^+ or LLS^+-FLAG without fractionation to confirm the smear pattern of LLS. Equivalent amounts of each fraction, corresponding to 100 µL of bacterial culture were separated on SDS-PAGE and submitted to immuno-detection, using the indicated antibodies. Data from one representative experiment out of the three performed are shown.

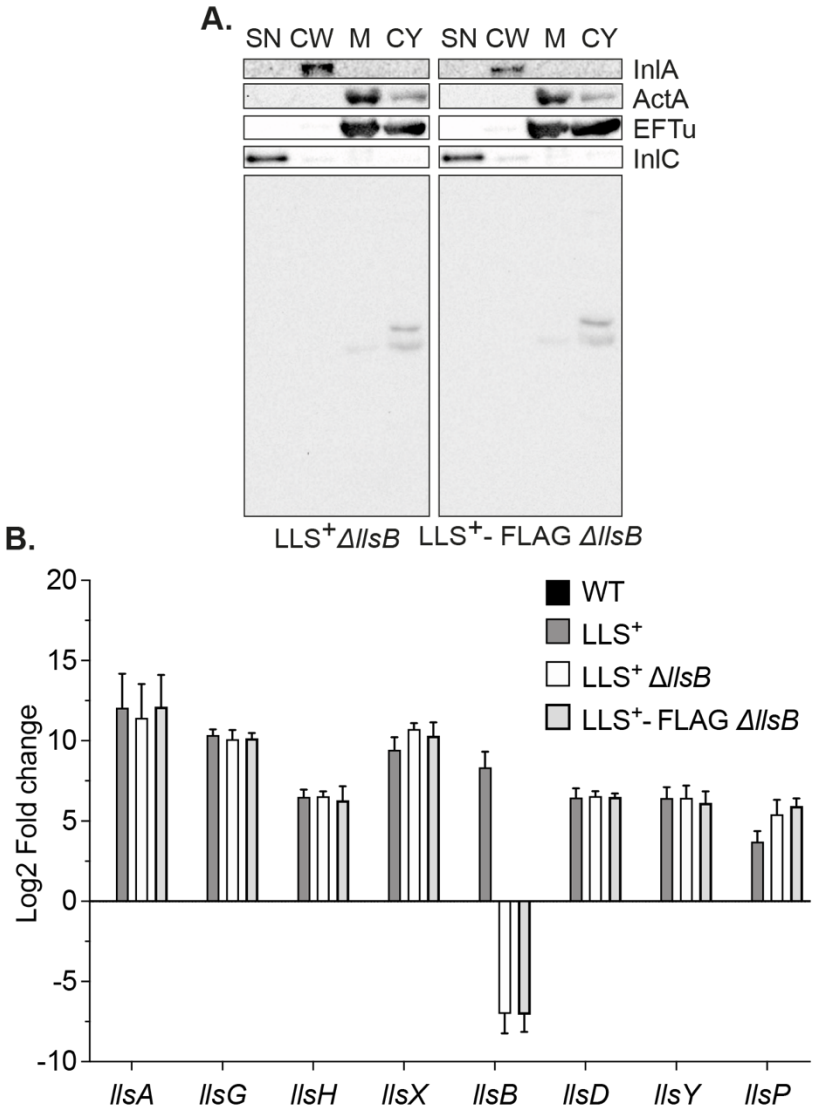

Figure S3. **Absence of LLS peptide and smear upon deletion of a putative subunit of the LLS post-translational machinery.** (A) Localization of LLS by fractionation experiments upon deletion of the *llsB* gene. Western Blot analysis was performed on LLS$^+$Δ*llsB* (negative control) and a LLS$^+$-FLAGΔ*llsB* strains. Proteins were fractionated in four compartments supernatant (SN), cell wall (CW), membrane (M) and cytoplasm (CY). InlA, ActA, EF-Tu and InlC were used as controls for fractionation. Equivalent amounts of each fraction, corresponding to 100 µL of bacterial culture were separated on SDS-PAGE and submitted to immuno-detection, using the indicated antibodies. Data from one representative experiment out of the three performed are shown. (B) Expression of the LLS genes *in vitro* in the *wt*, LLS$^+$ or LLS$^+$Δ*llsB* strains. Values calculated by qPCR in comparison with the *wt* strain and normalized to the housekeeping gene *gyrA* and represented as Log2 Fold change. Data from three independent biological experiments performed with three technical replicates are shown. Error bars show SEM.

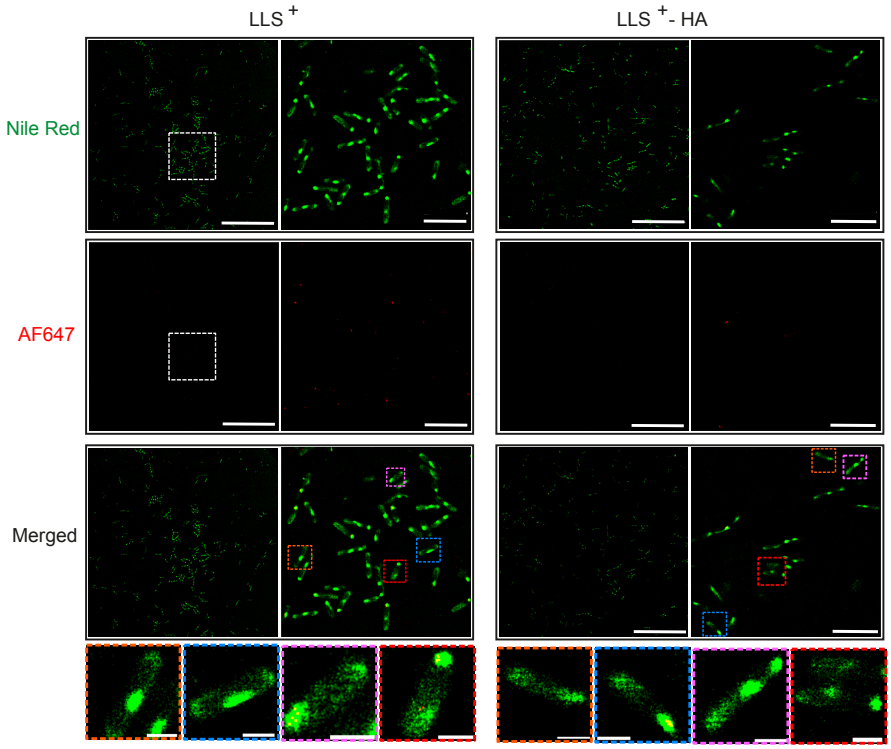

Figure S4. Super-resolution images of LLS$^+$-HA intact bacteria. Dual color super-resolution PAINT-dSTORM microscopy was performed on a strain expressing LLS$^+$ and a strain expressing LLS$^+$-HA. Bacteria were fixed and the bacterial membrane was imaged using PAINT with Nile Red dye (green). LLS was imaged using dSTORM microscopy with an AF647-conjugated anti-HA monoclonal antibody (red) (no specific signal associated to intact bacteria was detected). The left image shows a large FoV (scale bar 15 µm) and the right image a magnified view of the dashed white box (scale bar 3 µm). The colored dashed boxes show the Nile Red localizations labelling the membrane (scale bar 500 nm).

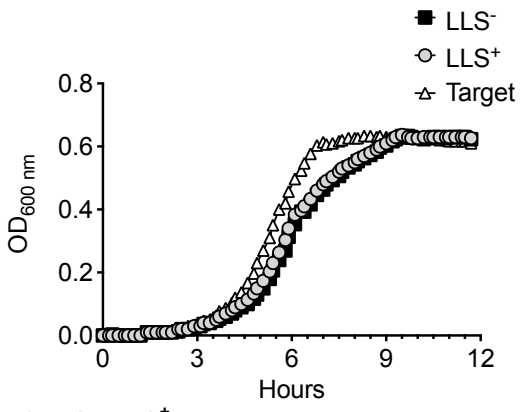

Figure S5. Growth curve of LLS$^-$, LLS$^+$ and target bacteria. *L. monocytogenes* F2365 (LLS$^-$ and LLS$^+$) and 10403S were grown in BHI media and OD_{600nm} measurements were taken every 20 min during 12 h in a Tecan's Sunrise absorbance microplate reader.

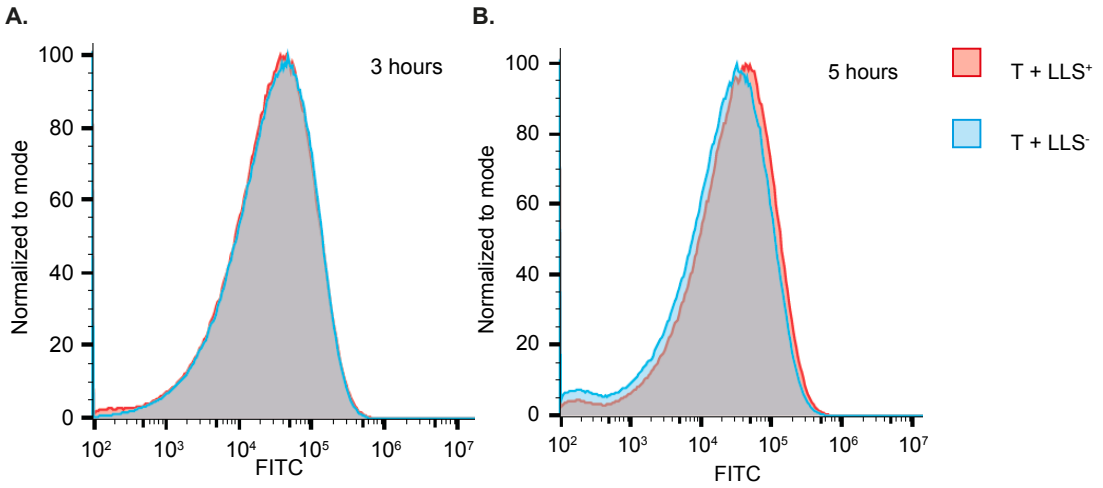

Figure S6. LLS does not affect the peptidoglycan synthesis of target cells. Click chemistry and flow cytometry analysis of 3-Azido D-Alanine labelled target bacteria (fluorescently labelled with Alexa fluor 594-alkyne via a copper-catalyzed click reaction). Labelled target bacteria were co-cultivated with LLS^- or LLS^+ cells during 3 h (A) and 5 h (B). Samples were acquired in a Cytoflex S and data were analyzed with FlowJo. Green fluorescence was collected from 40 000 FSC/SSC-gated bacterial events in the FITC channel and fluorescence intensities were plotted in single-parameter histograms that were normalized to mode for the two populations (target bacteria incubated with LLS^- or LLS^+). Data show one single experiment performed.

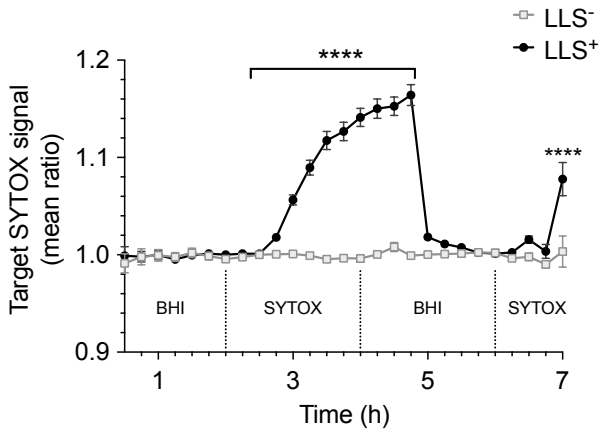

Figure S7. Recovery assays showing cell membrane permeabilization induced by LLS on target bacteria that are into contact with LLS producer bacteria. Time-lapse microscopy of LLS^+ or LLS^- and target bacteria over time. BHI medium was perfused during 2 h and then SYTOX blue dye was diluted in PBS and added after 2 h to label dying bacteria. To allow cells to resume growth a recovery assay was performed by perfusing BHI (2 h) and SYTOX dye (2 h) a second time as indicated. Quantification of SYTOX fluorescence intensity of target bacteria in contact with LLS^+ or LLS^- over time obtained from time-lapse microscopy. SYTOX fluorescence are obtained from R (shown in Fig. 3A) represented as ratios of intensities: mean. Data from one representative experiment out of the two performed are shown. Error bars show SEM. Multiple unpaired *t*-tests were performed. P values are significant from 3 h to 4 h 45 min and from 6 h 30 min until 7 h. (****$p< 0.0001$). LLS^- n=27 LLS^+ n=26.

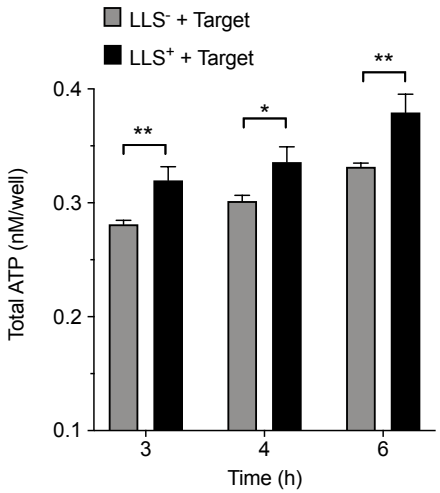

Figure S8. LLS induced release of ATP to the extracellular milieu. Total ATP levels present in culture supernatants after 3, 4 and 6 h of co-culture of *L. lactis* with LLS^+ or LLS^-. Data from one representative experiment out of the three performed are shown. Error bars show SEM. Multiple unpaired *t*-tests were performed (*$p<0.05$, **$p<0.01$).

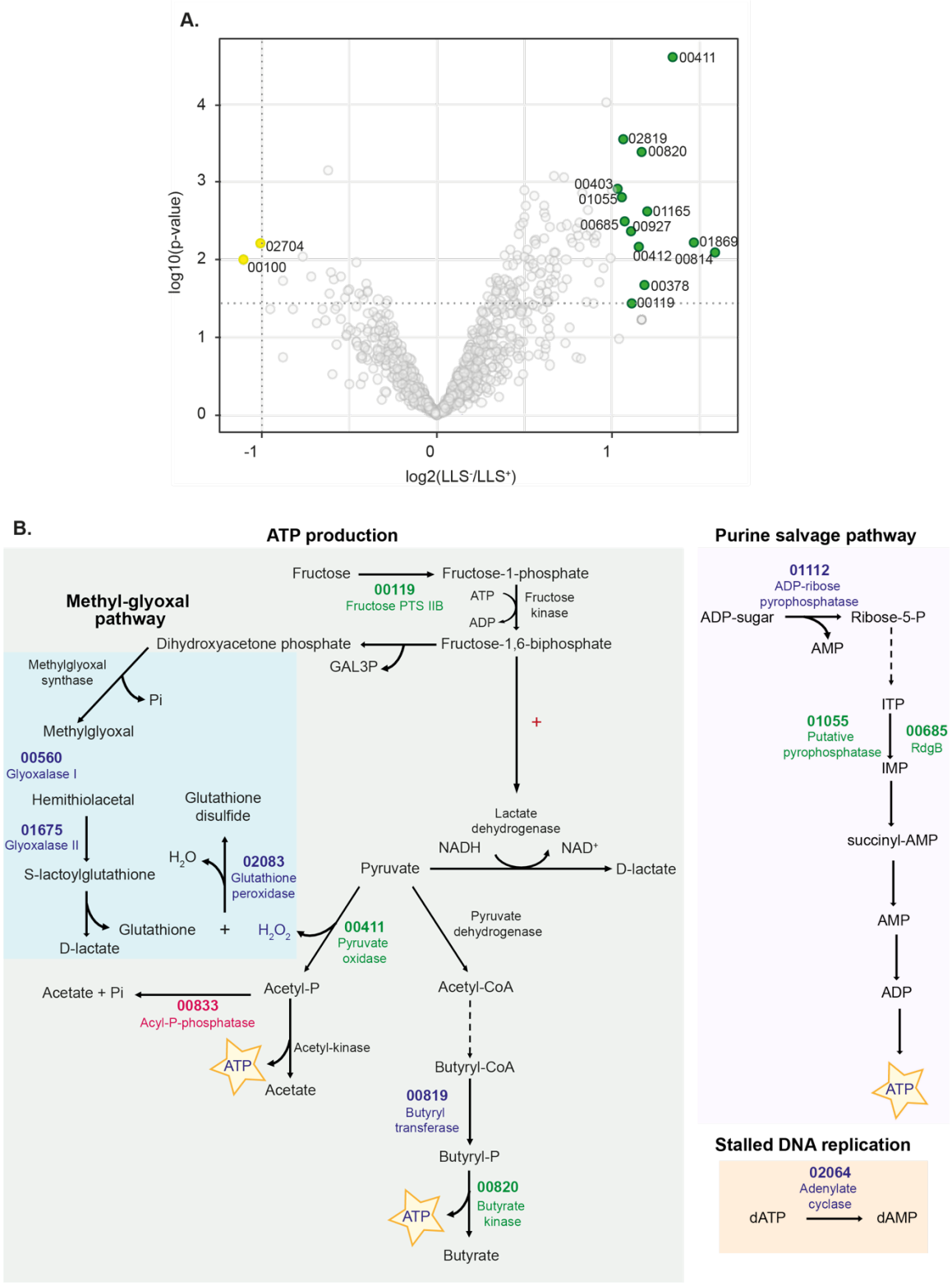

Figure S9. *Lm* 10403S proteins profile when co-cultivated with LLS$^+$ or LLS$^-$. (A) A volcano plot represents the set of differentially regulated proteins in response to a 4 hours co-culture with LLS$^+$ or LLS$^-$. Green (up-regulated) and yellow (down-regulated) circles are proteins with significantly altered expression in response to LLS$^+$, whereas gray points did not meet the q value (<0.01). *Lm* 10403S gene identifiers are indicated for the differentially upregulated and

downregulated proteins. (B) Representative proteins upregulated (in green) or exclusively expressed (in blue) in *Lm* 10403S when co-cultivated with LLS^+ or exclusively expressed in *Lm* 10403S when co-cultivated with LLS^- (in red). Black arrows represent direct reactions and dashed arrows indirect reactions. Experiments were performed 4 times independently.

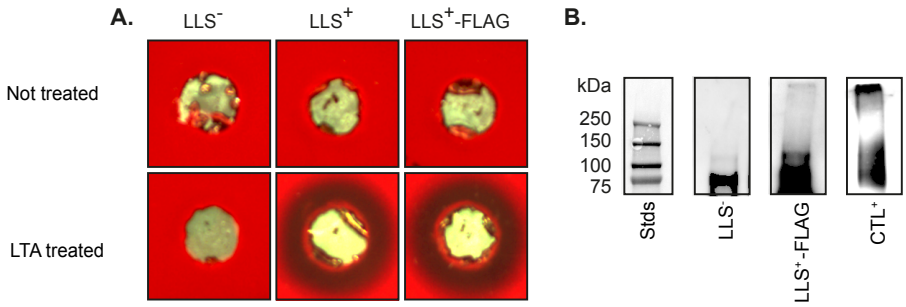

Figure S10. LLS can be extracted from the membrane of LLS$^+$ with LTA. (A) Assessment of hemolytic activity from bacteria-free supernatants extracted from the membrane of LLS$^+$ and LLS$^-$ strains (*hly*$^-$) by using purified LTA. (B) LTA induced extracts from LLS$^-$ and LLS$^+$-FLAG strains were immuno-precipitated by using magnetic beads coupled to anti-FLAG antibodies. Equivalent amounts of each fraction were separated on SDS-PAGE and submitted to immune-detection, using the anti-FLAG antibody. A membrane fraction from a LLS$^+$-FLAG strain was used as a positive control (CTL$^+$). The pre-stained protein standards (Stds) are shown at the left with the respective molecular weight in kDa. Data from one representative experiment out of the three performed are shown.

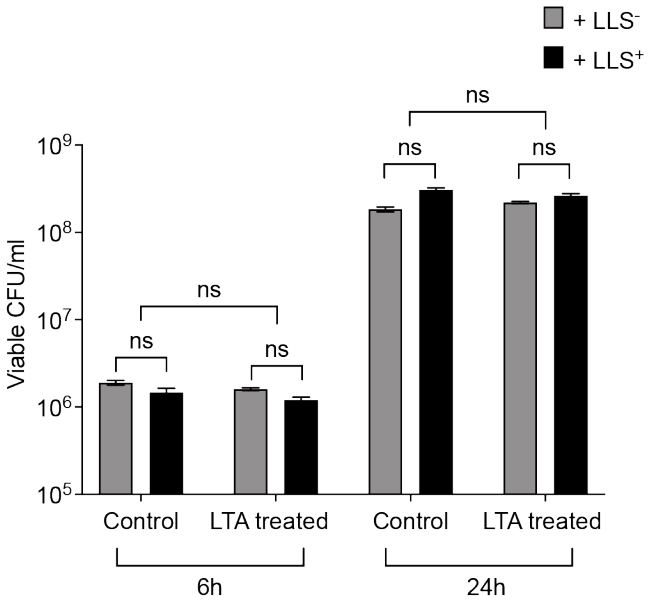

Figure S11. LTA-extracted supernatant fractions from LLS$^+$ *Lm* are not bactericidal. *L. lactis* target bacteria were cultivated for 6 h or 24 h with bacteria-free supernatants fractions extracted from the membrane of LLS$^+$ and LLS$^-$ *Lm* (*hly*$^-$) using purified LTA. Data from one representative experiment out of the three performed are shown. ns: no significant differences were observed between conditions.

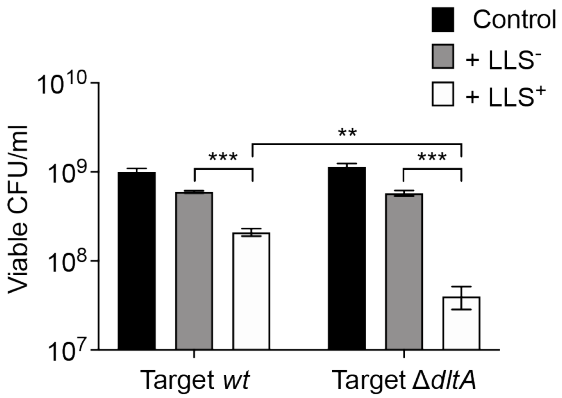

Figure S12. Target bacteria LTA decorations influence bacterial susceptibility to LLS. Target wt or Δ*dltA* EGD bacteria were cultivated alone or co-cultivated with LLS producer bacteria (LLS^+) or LLS mutant bacteria (LLS^-) during 24 h in BHI. Data from three independent biological experiments are shown. Error bars show SEM. Multiple two-tailed unpaired *t*-test were performed, wt LLS^+ vs LLS^- p= 0.0001, Δ*dltA* LLS^+ vs LLS^- p= 0.0002 and wt LLS^+ vs *dltA* LLS^+ p= 0.0018.

SI References

1. J. J. Quereda, *et al.*, Bacteriocin from epidemic *Listeria* strains alters the host intestinal microbiota to favor infection. *Proceedings of the National Academy of Sciences* **113**, 5706–5711 (2016).
2. C. U. Riedel, *et al.*, Improved Luciferase Tagging System for *Listeria monocytogenes* Allows Real-Time Monitoring In Vivo and In Vitro. *Applied and Environmental Microbiology* **73**, 3091–3094 (2007).
3. M. Arnaud, A. Chastanet, M. Debarbouille, New Vector for Efficient Allelic Replacement in Naturally Nontransformable, Low-GC-Content, Gram-Positive Bacteria. *Applied and Environmental Microbiology* **70**, 6887–6891 (2004).
4. D. Balestrino, *et al.*, Single-Cell Techniques Using Chromosomally Tagged Fluorescent Bacteria To Study *Listeria monocytogenes* Infection Processes. *Applied and Environmental Microbiology* **76**, 3625–3636 (2010).
5. J. Mengaud, *et al.*, Antibodies to the leucine-rich repeat region of internalin block entry of *Listeria monocytogenes* into cells expressing E-cadherin. *Infect. Immun.* **64**, 5430–5433 (1996).
6. P. Steffen, *et al.*, *Listeria monocytogenes* ActA protein interacts with phosphatidylinositol 4,5-bisphosphate in vitro. *Cell Motil. Cytoskeleton* **45**, 58–66 (2000).
7. R. Boujemaa-Paterski, *et al.*, *Listeria* Protein ActA Mimics WASP Family Proteins: It Activates Filament Barbed End Branching by Arp2/3 Complex. *Biochemistry* **40**, 11390–11404 (2001).
8. C. Archambaud, E. Gouin, J. Pizarro-Cerda, P. Cossart, O. Dussurget, Translation elongation factor EF-Tu is a target for Stp, a serine-threonine phosphatase involved in virulence of *Listeria monocytogenes*: EF-Tu, a target for the Listeria phosphatase Stp. *Molecular Microbiology* **56**, 383–396 (2005).
9. E. Gouin, *et al.*, The *Listeria monocytogenes* InlC protein interferes with innate immune responses by targeting the I B kinase subunit IKK. *Proceedings of the National Academy of Sciences* **107**, 17333–17338 (2010).
10. J. R. Mellin, *et al.*, Sequestration of a two-component response regulator by a riboswitch-regulated noncoding RNA. *Science* **345**, 940–943 (2014).
11. M. Lelek, *et al.*, Superresolution imaging of HIV in infected cells with FlAsH-PALM. *Proceedings of the National Academy of Sciences* **109**, 8564–8569 (2012).
12. M. Lelek, F. Di Nunzio, C. Zimmer, "FlAsH-PALM: Super-resolution Pointillist Imaging with FlAsH-Tetracysteine Labeling" in *Exocytosis and Endocytosis*, Methods in Molecular Biology., A. I. Ivanov, Ed. (Springer New York, 2014), pp. 183–193.
13. M. Ovesný, P. Křížek, J. Borkovec, Z. Svindrych, G. M. Hagen, ThunderSTORM: a comprehensive ImageJ plug-in for PALM and STORM data analysis and super-resolution imaging. *Bioinformatics* **30**, 2389–2390 (2014).
14. R. Jonquières, H. Bierne, F. Fiedler, P. Gounon, P. Cossart, Interaction between the protein InlB of *Listeria monocytogenes* and lipoteichoic acid: a novel mechanism of protein association at the surface of gram-positive bacteria. *Mol. Microbiol.* **34**, 902–914 (1999).
15. J. Schindelin, *et al.*, Fiji: an open-source platform for biological-image analysis. *Nat Methods* **9**, 676–682 (2012).
16. D. Legland, I. Arganda-Carreras, P. Andrey, MorphoLibJ: integrated library and plugins for mathematical morphology with ImageJ. *Bioinformatics*, btw413 (2016).
17. F. de Chaumont, *et al.*, Icy: an open bioimage informatics platform for extended reproducible research. *Nat Methods* **9**, 690–696 (2012).
18. I. Santi, N. Dhar, D. Bousbaine, Y. Wakamoto, J. D. McKinney, Single-cell dynamics of the chromosome replication and cell division cycles in mycobacteria. *Nat Commun* **4**, 2470 (2013).
19. S. Wieczorek, *et al.*, DAPAR & ProStaR: software to perform statistical analyses in quantitative discovery proteomics. *Bioinformatics* **33**, 135–136 (2017).
20. Q. Giai Gianetto, S. Wieczorek, Y. Couté, T. Burger, "A peptide-level multiple imputation strategy accounting for the different natures of missing values in proteomics data" (Bioinformatics, 2020) https:/doi.org/10.1101/2020.05.29.122770 (September 18, 2020).
21. M. E. Ritchie, *et al.*, limma powers differential expression analyses for RNA-sequencing and microarray studies. *Nucleic Acids Research* **43**, e47–e47 (2015).
22. Q. Giai Gianetto, *et al.*, Calibration plot for proteomics: A graphical tool to visually check

the assumptions underlying FDR control in quantitative experiments: Calibration Plot for Proteomics (CP4P). *Proteomics* **16**, 29–32 (2016).
23. S. Pounds, C. Cheng, Robust estimation of the false discovery rate. *Bioinformatics* **22**, 1979–1987 (2006).
24. J. E. Alouf, C. Loridan, “Production, purification, and assay of streptolysin S” in *Methods in Enzymology*, (Elsevier, 1988), pp. 59–64.
25. M. J. Linnan, *et al.*, Epidemic Listeriosis Associated with Mexican-Style Cheese. *New England Journal of Medicine* **319**, 823–828 (1988).
26. J. J. Quereda, *et al.*, Listeriolysin S Is a Streptolysin S-Like Virulence Factor That Targets Exclusively Prokaryotic Cells In Vivo. *mBio* **8**, e00259-17, /mbio/8/2/e00259-17.atom (2017).
27. D. K. Bishop, D. J. Hinrichs, Adoptive transfer of immunity to *Listeria monocytogenes*. The influence of in vitro stimulation on lymphocyte subset requirements. *J. Immunol.* **139**, 2005–2009 (1987).
28. E. G. D. Murray, R. A. Webb, M. B. R. Swann, A disease of rabbits characterised by a large mononuclear leucocytosis, caused by a hitherto undescribed bacillus *Bacterium monocytogenes* (n.sp.). *J. Pathol.* **29**, 407–439 (1926).
29. P. Mandin, *et al.*, VirR, a response regulator critical for *Listeria monocytogenes* virulence: Novel *Listeria* virulence regulon. *Molecular Microbiology* **57**, 1367–1380 (2005).
30. B. Périchon, *et al.*, Regulation of PI-2b Pilus Expression in Hypervirulent Streptococcus agalactiae ST-17 BM110. *PLoS ONE* **12**, e0169840 (2017).
31. S. Arous, *et al.*, Global analysis of gene expression in an rpoN mutant of Listeria monocytogenes. *Microbiology* **150**, 1581–1590 (2004).
32. Y. Okada, *et al.*, The sigma factor RpoN (sigma54) is involved in osmotolerance in Listeria monocytogenes. *FEMS Microbiol Lett* **263**, 54–60 (2006).
33. R. Gutknecht, The dihydroxyacetone kinase of Escherichia coli utilizes a phosphoprotein instead of ATP as phosphoryl donor. *The EMBO Journal* **20**, 2480–2486 (2001).
34. B. Troxell, H. M. Hassan, Transcriptional regulation by Ferric Uptake Regulator (Fur) in pathogenic bacteria. *Front. Cell. Infect. Microbiol.* **3** (2013).